

The Jinxian Biota revisited: taphonomy and body plan of the Neoproterozoic discoid fossils from the southern Liaodong Peninsula, North China

Cui Luo^{1,3} · Maoyan Zhu² · Joachim Reitner³

Received: 15 October 2014 / Accepted: 17 January 2016 / Published online: 3 February 2016
© Paläontologische Gesellschaft 2016

Abstract The fossil record indicates that complex multicellular organisms started to become dominant in the second half of the Neoproterozoic. However, many macroscopic fossils of this period are not yet well understood. As one example, the Jinxian Biota includes some affinity-unresolved, millimeter- to centimeter-sized discoid fossils of probable pre-Ediacaran age from the shales of the Xingmincun Formation, in southern Liaodong Peninsula, China. This paper presents new observations of these fossils based on new material. Three types of preservation were identified and analyzed. The organisms were probably transported by turbidity currents, rapidly buried in fine-grained deposits and then compacted to yield thin films. Pyrite- and carbonate-related mineralization may have been involved in their early diagenesis, but local-controlled late diagenesis altered the fossil-related mineral composition to that observed today. The concentric annular relief on the fossil surfaces exhibits a “half convex, half

concave” pattern, which is interpreted to reflect the differentiated mechanical nature between adjacent annuli. New specimens have been found that support the existence of programmed fission and budding. In addition, another group of previously ignored discoid fossils are first described here. With the same preservation as the “normal” discs, these fossils lack any concentric relief and always occur in clusters. The relationship between the two types of discs remains unclear. Even with all of the new information, it remains impossible to indubitably correlate the Jinxian Biota to any known taxonomic group. However, it is quite probable that these fossils represent a group of eukaryotic organisms.

Keywords Neoproterozoic · Discoid fossils · Taphonomy · Xingmincun formation · North China

Kurzfassung Der fossile Bericht zeigt, dass größere komplexe Organismen erst in der zweiten Hälfte des Neoproterozoikums (Cryogenium) erscheinen. Allerdings sind diese Fossilien nur schwer interpretierbar und es ist nicht möglich sie heutigen Metazoen zu zuordnen. Ein Beispiel dafür sind die bis einige Zentimeter großen scheibenförmigen Fossilien aus der Xingmincun Formation (südliche Liaodong Halbinsel, Nordchina). In der vorliegenden Arbeit werden neue Beobachtungen zur Paläobiologie dieser Fossilien beschrieben basierend auf drei unterschiedlichen Erhaltungsstadien. Die Organismen wurden sehr wahrscheinlich in Suspensionswolken von feinkörnigen Mikroturbiditen transportiert und durch diesen Prozess rasch im Sediment eingebettet. Durch diesen Vorgang wurden sie zu dünnen Scheiben kompaktiert. Es lassen sich drei unterschiedliche Erhaltungstypen, bedingt durch unterschiedliche diagenetische Bedingungen, unterscheiden. Die drei verschiedenen Diagenestypen

Electronic supplementary material The online version of this article (doi:10.1007/s12542-016-0289-5) contains supplementary material, which is available to authorized users.

✉ Cui Luo
cluoms@outlook.com

- ¹ Key Laboratory of Economic Stratigraphy and Palaeogeography, Nanjing Institute of Geology and Palaeontology, Chinese Academy of Sciences, 39 East Beijing Road, 210008 Nanjing, China
- ² State Key Laboratory of Palaeobiology and Stratigraphy, Nanjing Institute of Geology and Palaeontology, Chinese Academy of Sciences, 39 East Beijing Road, 210008 Nanjing, China
- ³ Department of Geobiology, Centre of Geosciences of the University of Göttingen, Goldschmidtstraße 3, 37077 Göttingen, Germany

unterscheiden sich in den assoziierten Mineralien und in der Dicke der Scheiben. Die Scheiben zeigen konzentrische, reliefartige Muster mit halb konvexen und halb konkaven Kompaktionsstrukturen. Neben diesen spezifischen Oberflächenstrukturen finden sich Teilungs- und Knospungsmuster. Es wird eine weitere Form dieser Scheiben-Fossilien beschrieben, die keine konzentrischen Strukturen aufweisen und stets zusammen mit vielen Individuen auftreten (Schwarm). Die vorgestellten Fossilien zeigen gute Übereinstimmungen mit den “*Beltanelliformis*” Fossilien der unterkambrischen Pusa Formation in Spanien. Eine engere taxonomische Zuordnung zu einem bekannten Taxon konnte bis dato nicht vorgenommen werden.

Schlüsselwörter Neoproterozoikum · Diskus-förmige Fossilien · Taphonomie · Xingmuncun Formation · Nordchina

Introduction

Although simple forms of multicellularity can be traced back to the Mesoproterozoic (e.g., Butterfield 2009), the Cryogenian and Ediacaran periods are likely the most important for observing the rise of real complex multicellular life forms (e.g., Narbonne et al. 2012; Shields-Zhou et al. 2012). However, as exemplified by the famous but puzzling Ediacara Biota, many Cryogenian and Ediacaran macroscopic fossils are difficult to assign to known taxonomic groups. In some cases, it is even unclear whether a macroscopic fossil represents a true multicellular organism or a special microbial structure. Discoid fossils are undoubtedly one of these problematic groups (MacGabhann 2007). Progress in deciphering these enigmatic fossils may enhance our understanding of the ancient biosphere and its evolution during this critical interval of Earth history.

First described by Hong et al. (1988), the “Jinxian Biota” represents a group of enigmatic discoid fossils from the Precambrian Xingmuncun Formation in southern Liaodong Peninsula, North China. According to the first description, these fossils are circular to elliptical discs with diameters of 5–28 mm that exhibit concentric annuli and radial structures and are covered by a mineral sheet consisting of quartz and chlorite. They were then interpreted as distinct local cnidarian medusae and assigned into three genera and six species. Subsequent studies have expressed different viewpoints on the classification and biological interpretation of these fossils, regarding them as either analogues of Ediacaran discs (Niu et al. 1988) or hydrozoan medusa (Wang 1991). However, the preservation of these fossils was not closely investigated until the study

conducted by Zhang et al. (2006). These researchers studied the microscopic structures of the mineral “membranes” defining the fossils and determined that some structures of the chlorite sheaths resemble a biofilm. Additionally, these researchers provided the first demonstration of various biological or burial-related features of these fossils, including overlapping, folding, possible fission, and the unique spiral relief observed in some specimens. Based on their analysis, these researchers concluded that the Jinxian Biota is distinct from any known fossil or living organisms. The recent study conducted by Ou and Meng (2013) analyzed the size distribution of 221 specimens from the Jinxian Biota, and the results show a left-skewed size distribution toward the smaller end, similar to that of *Aspidella*, a characteristic component of many Ediacaran localities (Peterson et al. 2003).

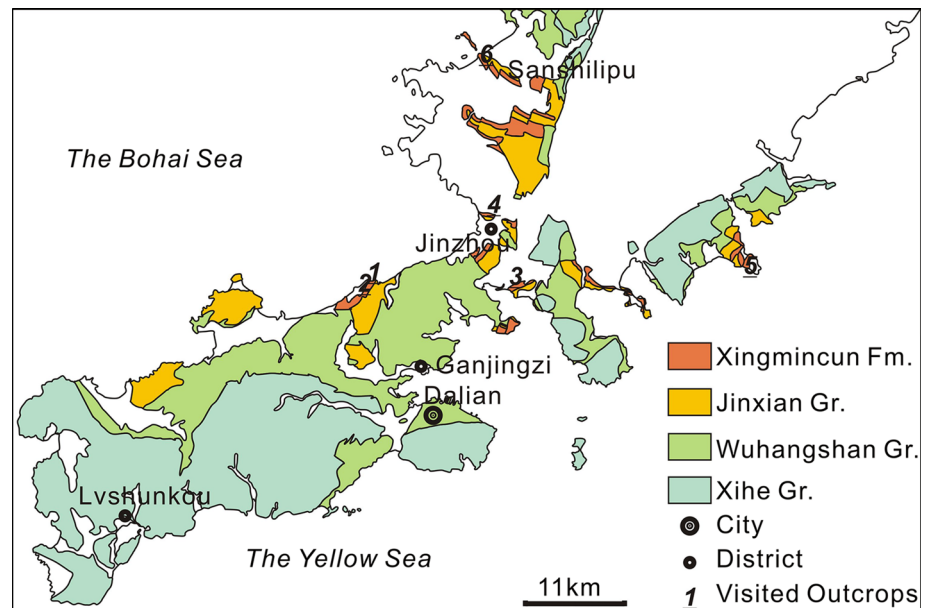
Our investigation presented here provides some previously unreported taphonomic and morphological details. These observations improve our current understanding of the nature of these enigmatic fossils and in turn increase our knowledge of the Neoproterozoic biosphere.

Material and geological setting

Six outcrops of the Xingmuncun Formation were visited in 2009 and 2010, but fossils were only discovered in three of them (Fig. 1). All of the collected rock and fossil samples are deposited at the Nanjing Institute of Geology and Palaeontology, Chinese Academy of Sciences (NIGPAS).

The Xingmuncun Formation is a lithological unit close to the top of the Precambrian succession in the Jinzhou-Dalian area (Fig. 2). The subdivision of the local Precambrian sedimentary succession varies depending on the researcher. Following the scheme proposed by Hong et al. (1991), this succession is composed of the Yongning, Xihe, Wuhangshan, and Jinxian groups in ascending order. The Xingmuncun Formation belongs to the Jinxian Group and is overlain by the Getun Formation, which in turn overlies the Cambrian Dalinzi Formation (Fig. 2). However, this placement of the Precambrian-Cambrian boundary is only one of the existing resolutions. Other researchers place this boundary either between the Xingmuncun and Getun Formations (Duan and An 1994; Qiao et al. 2001) or at the top of the Dalinzi Formation (Xue et al. 2001). In fact, in neither the Dalinzi nor the Getun Formation have any indisputable Cambrian fossils ever been discovered, whereas the Jianchang Formation, which unconformably overlies the Dalinzi Formation, belongs to the Canglangpuian (Botomian to Toyonian) according to trilobite and archaeocyath assemblages (Hong et al. 1990). In addition

Fig. 1 Spacial distribution of the Precambrian sedimentary rocks in the Jinzhou-Dalian area (according to the Geological Survey Group of Liaoning Province 1972). The visited outcrops of the Xingmincun Formation are marked with numbers: 1 Qipanmo section; 2 Yangjuanzi section; 3 Yangtun section; 4 Beishan section; 5 Jinshitan section; 6 Luhai section



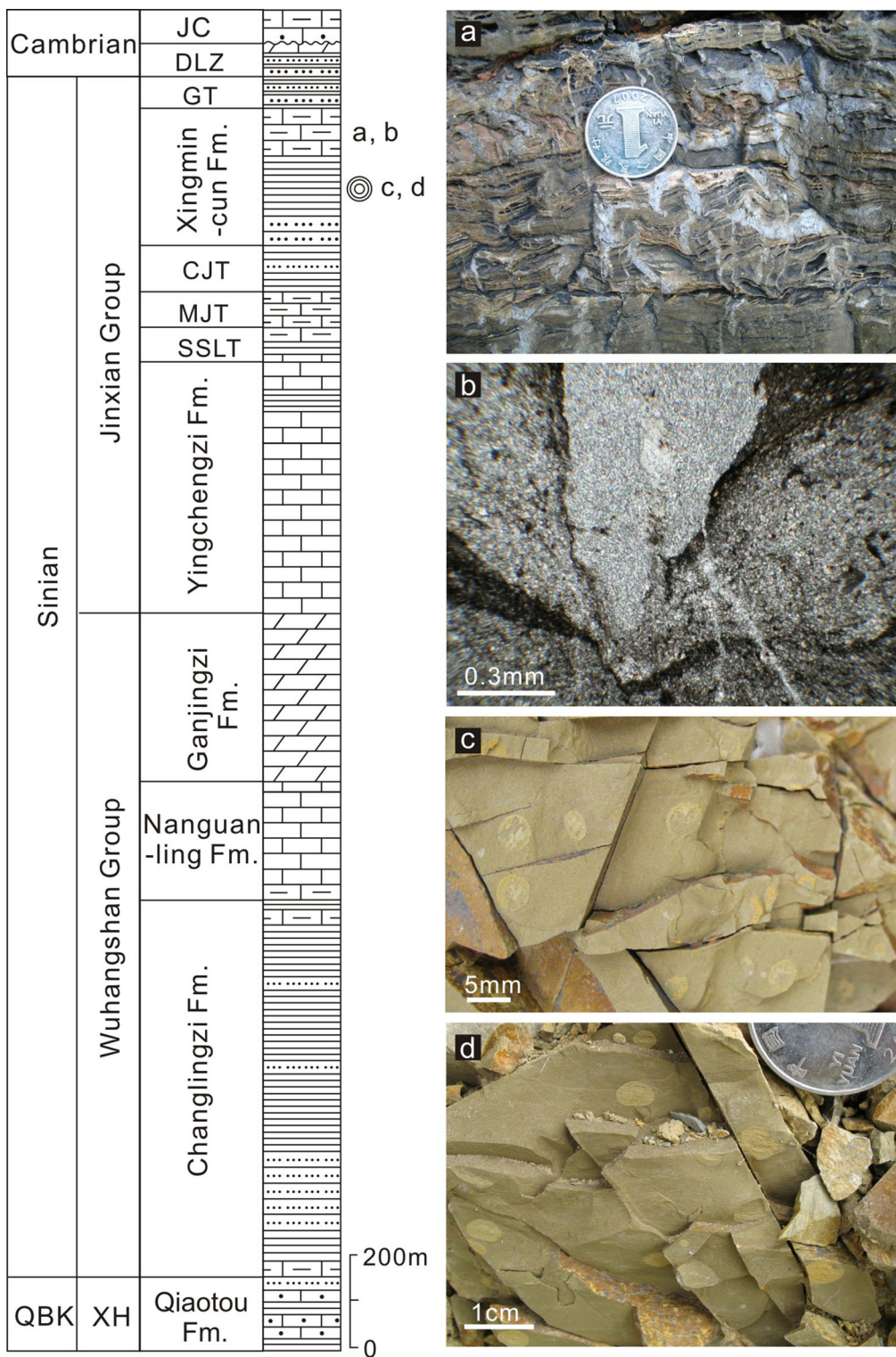
to the uncertainty of its relation to the Precambrian-Cambrian boundary, the radiometric dating of the Xingmincun Formation also yields incongruent results, ranging from a K–Ar age of approximately 579 Ma to a Rb–Sr age of approximately 650–677 Ma (Xing et al. 1989; Hong et al. 1991). However, other lithostratigraphic (Cao et al. 1988; Xue et al. 2001) and chemostratigraphic correlations (Fairchild et al. 2000; Zheng et al. 2004; Shields-Zhou, personal communication) suggest that this rock unit is older than the Ediacaran. Recently obtained U–Pb ages from detrital zircons from the Lower Xingmincun Formation constrain the age of this formation to younger than 924 Ma (Yang et al. 2012), whereas a newly published integrated correlation places this formation in the Tonian (Xiao et al. 2014). Consistent with these correlations, molar tooth structures are observed in the upper unit of the Xingmincun Formation (Fig. 2a, b). Massive occurrences of these structures are mainly known from rocks older than 700 Ma with only one Ediacaran exception (Shields et al. 2002). Acritarchs reported from this formation are dominated by structureless leiosphaerids with minor fusiforms (e.g., Yang 1984; Qiao et al. 2001).

The sedimentary record of the Xingmincun Formation generally exhibits a transgressive sequence consisting of glauconite-containing sandstone in the lower part, mudstone in the middle part, and limestone in the upper part (Fig. 2). According to previous studies and the present investigation, the discoid fossils are exclusively preserved in the mudstone unit. Among the six visited outcrops of the Xingmincun Formation, only the Qipanmo, Yangjuanzi, and Yangtun sections were found to be fossiliferous (Fig. 1). The Qipanmo section is severely affected by

Triassic dolerite intrusions and modern artificial covering, and is thus not suitable for sedimentological observation. The Yangjuanzi section shows better preserved sedimentary structures. The fossil-bearing rocks are composed of siltstone-mudstone cycles separated by erosion surfaces at the base of the siltstone layers, and the discoid fossils are preserved in the muddy parts only (Fig. 3b–d). These sediments are characteristic of turbidites because they show an erosional surface succeeded by a silty subunit which is abruptly overlain by intercalated silt/clay laminae and then a clay drape (Fig. 3c). The Yangtun section extends along a canal, with its bedding trending approximately parallel to the canal wall. Although lacking a direct transverse profile, the sedimentological features of this section resemble those observed in the Yangjuanzi section, i.e., multiple stacked cycles consisting of a silty subunit and an overlying fossiliferous muddy subunit.

Methods

Fossil specimens and relevant petrographic thin sections were first checked using a LEICA MZ-16A stereomicroscope, a Leitz Ortholux polarizing microscope and a ZEISS Axioskop biomicroscope. To study the mineral composition of the fossils, a LEO 1530VP scanning electron microscope (SEM) equipped with an energy dispersive X-ray spectrometer (EDS) in the State Key Laboratory of NIGPAS and a JY HR800 laser Raman spectroscope with a 488-nm laser source in the Centre of Modern Analysis, Nanjing University, were utilized. The resulting Raman spectra were analyzed using the Crystal Sleuth software. Its



Legends

- sandstone siltstone shale sandy limestone
- muddy limestone limestone dolomite discoid fossils

◀ **Fig. 2** Stratigraphy of the Precambrian sedimentary rocks on the southern Liaodong Peninsula. The stratigraphic column was modified from Zhang et al. (2006), and the lithostratigraphic subdivision follows the scheme proposed by Hong et al. (1991). **a, b** Molar tooth structures from the limestones in the upper part of the Xingmincun Formation in the Jinshitan section; the diameter of the coin is 25 mm. **c, d** Fossil-bearing mudstones of the middle Xingmincun Formation in the Yangtun section. *CJT* Cuijiatun Formation, *DLZ* Dalinzi Formation, *GT* Getun Formation, *JC* Jianchang Formation, *MJT* Majiatun Formation, *QBK* Qingbaikou System, *SSLT* Shisanlitai Formation, *XH* Xihe Group

pre-compiled spectra database was provided by the RRUFF™ Project. The fossil size and diameter of the concentric relief structures were measured directly under the stereomicroscope, whereas the thicknesses of these fossils were obtained from scaled photos taken through optical microscope and SEM.

Results

General description

The discoid fossils can be easily identified from the host rocks because of their yellow, green, or greenish-grey coloration, which is related to the different mineral compositions within the fossil region (Figs. 4, 5; details see “Preservation”). These fossils are preserved as flattened discs with explicit, smooth margins, and most of them have a circular or elliptical outline with diameters ranging from a few millimeters to approximately 2.5 cm (Fig. 5d–f). Elliptical specimens may or may not exhibit a preferred alignment (Fig. 2c, d). Relatively rare heart-, sausage-, clover- and even irregularly shaped individuals were also observed (Fig. 4j–n). In the transverse section, the discoid fossils appear as wrinkled bodies embedded in the muddy host rock, and each shows a uniform thickness in the middle part and tapers toward the two ends (Figs. 5g, h, 6a, b). These fossils are either parallel (e.g., Fig. 3c) or oblique (e.g., Fig. 4f) to the bedding plane at various angles.

The fossils of both disc-like and irregular forms exhibit different numbers of concentric annuli (relief structures). Each annulus is notably concave in one half of the circle and convex in the other half (e.g., Figs. 4i, 11a, b). The distribution of the annuli on the fossil surface can be irregular. In some specimens, the annuli may skew toward a specific direction (Fig. 4h), or the elliptical annuli in one individual show differently oriented long axes (Fig. 4b). Radial structures are present only in few specimens and appear to be a product of compaction (Fig. 4c). Spiral ridges, like those described by Zhang et al. (2006), were not observed. However, a few of our specimens show structures similar to spiral ridges when illuminated at a

particular angle (Fig. 4g, o, p). A few specimens have a small pimple (diameter <1 mm) in the center of the disc (e.g., Fig. 4a, i, p), which appears to be a biological structure of the original organism, although its function is unclear. Some fossils are overprinted by directional wrinkles that are less prominent in the surrounding mudstone (e.g., Fig. 4j, k, m, n). These wrinkles were probably formed in early diagenesis, when the sediments were non-lithified and the carcasses were not fossilized. The deformation was better recorded by the fossils than by the sediments because the muddy sediments were homogeneous and the sedimentary particles were movable at that time.

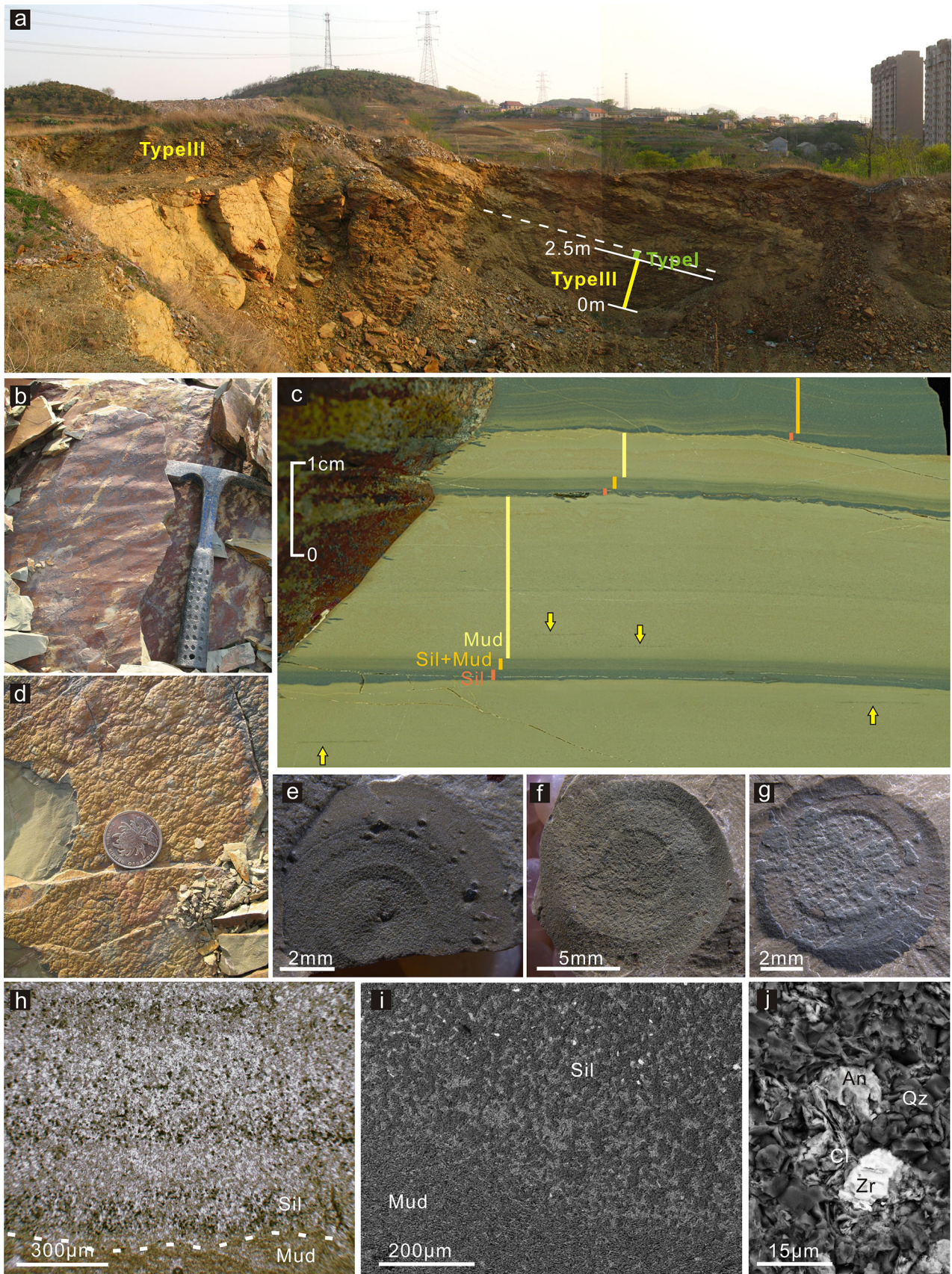
Because of the above-described features, particularly the soft-bodied deformations that have been demonstrated by Zhang et al. (2006) and will be amended and expanded in this paper, the biogenic nature of these discoid structures has not been questioned since their first description provided by Hong et al. (1988).

Preservation

In this study, the discoid fossils of the Jinxian Biota were found to show more varieties of preservation than previously reported. According to the associated mineralogy and compaction of the fossils, three preservation types were identified and are described below.

Preservation type I

This is the only type of preservation that has previously been studied in detail (Hong et al. 1988; Tang 1997; Zhang et al. 2006). Specimens of this preservation type are defined by a smooth, green to dark green mineral sheet, and their concentric relief structures are preserved as strong and prominent grooves and ridges (Fig. 5a). The mineral sheet is composed of a layer of quartz crystallites with a clay mineral sheath that was previously found to be composed of chlorite (Hong et al. 1988; Tang 1997; Zhang et al. 2006). This clay mineral sheath appears distinct from the minerals in the host rock when viewed with the naked eye (Fig. 5a) or sometimes with an optical microscope (Figs. 5g, 6a), and even by backscattered electron imaging under low magnification. However, when observed at higher SEM magnifications (Fig. 7d), by elemental mapping (Fig. 7g), or through Raman spectroscopy (Fig. 6c), the clay sheaths are indistinguishable from the host rock. Additionally, some specimens, which are not prone to be knocked out of the mudstone, do not show any identifiable clay mineral sheath surrounding the quartz layer under an optical microscope (Fig. 5h). In many cases, the quartz crystallites decrease in size from the center of the mineral sheet to its edge (Fig. 7b). Those structures resembling



◀ **Fig. 3** Sedimentary features of the Yangjuanzi section. **a** An overview of the outcrop, with an illustration of the vertical distribution of different fossil preservation types. **b** Flute cast on the bedding plane; the length of the hammer is approximately 30 cm. **c** A polished transverse section showing the siltstone-mudstone sedimentary cycles; the *arrows* point to fossils. **d** Load cast on the sole of a silty layer; the coin diameter is 25 mm. **e–g** From *left to right*: preservation type III gradually grades into type I. Specimen numbers: **e** No. 10284, **f** No. 10296, **g** No. 10209. **h** The boundary between muddy and silty layers in a thin section. **i** The boundary between muddy and silty layers under SEM (backscattered electron). The *upper-right* part is the silty layer, and the *lower-left* part is the muddy layer. The darkest minerals in the *upper-left* part are quartz, the minerals with medium brightness are silicates, and the brightest grains are heavy minerals. **j** A closer view of the heavy minerals. *An* anatase, *Cl* clay minerals, *Mud* mudstone, *Sil* siltstone, *Qz* quartz, *Zr* zircon

microbial films that were previously reported by Zhang et al. (2006) were not detected in this study. Instead, the mineral sheets are likely of abiotic origin, as a similar mineralogical composition was also observed in the fracture-fillings in one of our samples (Fig. 7e, f). This preservation type was found in both the Qipanmo and Yangjuanzi sections, and in the latter, it continuously grades into preservation type III (Fig. 3a, e–g).

Preservation type II

These specimens are defined by a thin, yellow layer of mineral grains, and the concentric reliefs are preserved as strong and prominent grooves and ridges (Fig. 5b). The mineral grains on the fossil surface do not form a continuous sheet such as that observed with preservation type I. When viewed in the transverse section, the fossil body appears as a pre-existed cavity, and the minerals appear to be the related pore-fillings, growing from the wall of the cavity toward its center (Fig. 7h–k). These pore-fillings include a large amount of Fe-rich clay minerals (Fig. 7j) and anatase (Figs. 6d, 8b), with less quartz and few apatite crystals (Fig. 8c). Because of this mineral composition, the entire fossil surface is rich in Fe and Ti, as determined through elemental mapping (Fig. 8d). This preservation type was found only in the Yangtun section. Irregularly shaped specimens are markedly more common in this section than in the other outcrops.

Preservation type III

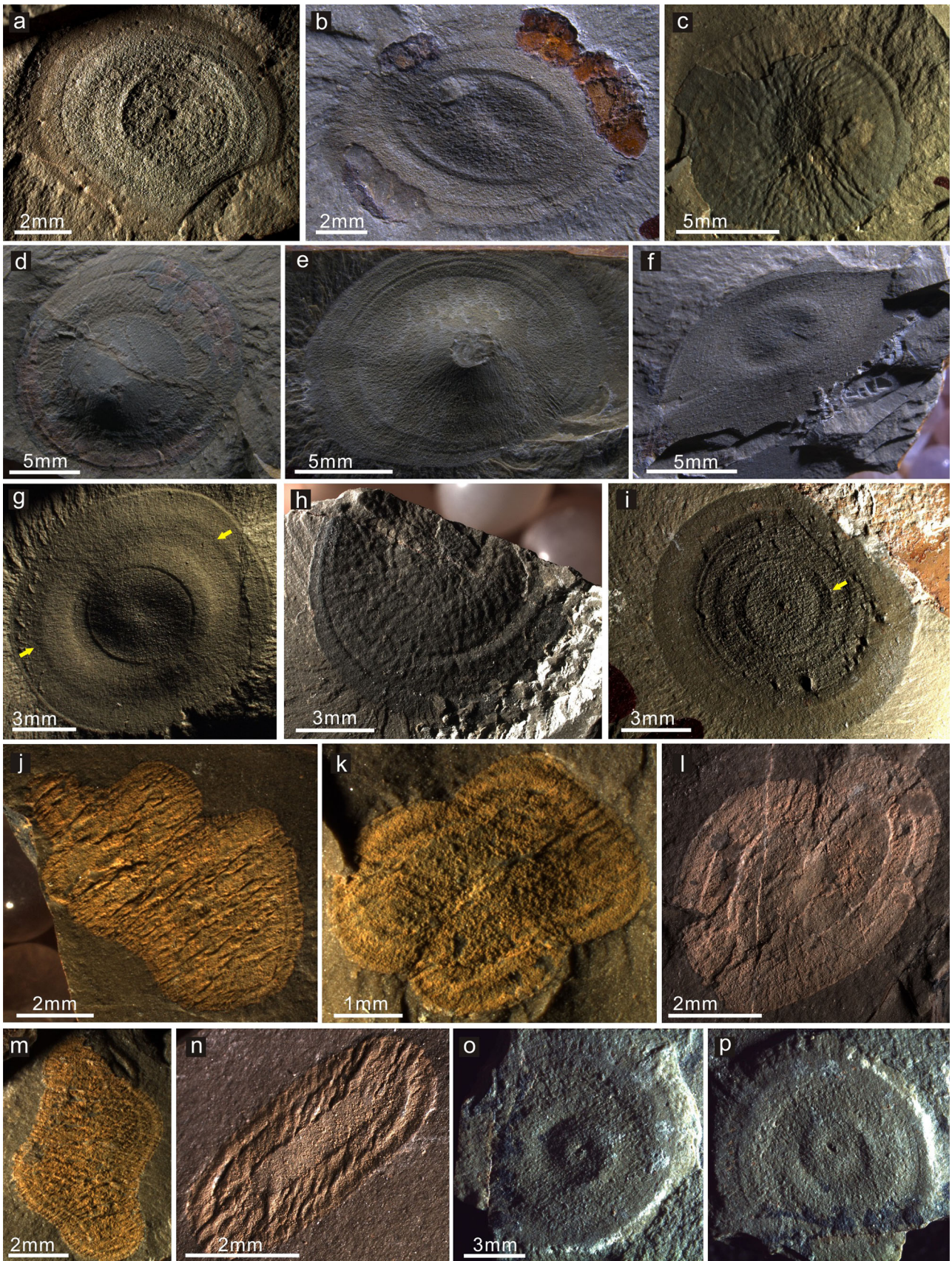
Specimens of this preservation type lack a visible mineral covering on the surface but still stand out from the host rock due to their slightly different color and/or surface roughness (Fig. 5c). The concentric reliefs are preserved in a very fine and delicate way. In the transverse section, the fossils are too thin to recognize. In this study, two

examples were examined in transverse section because their surfaces are partly exposed in the hand specimen. Both specimens are less than 10- μ m thick and show only a few quartz grains in the fossil-related space (Fig. 7c). However, as determined through elemental mapping, most fossils of preservation type III show a significant enrichment of Fe on the surface (Fig. 8h), probably due to the accumulation of Fe-rich clay minerals (Fig. 8g). Clusters of needle-shaped iron oxide minerals were observed in the weathered part of some specimens (Fig. 8e, f), and interestingly, some of these mineral clusters are dumbbell-shaped. This preservation type is found mainly in the Yangjuanzi section, where it continuously grades into preservation type I (Fig. 3a, e–g). In the Qipanmo section, a fallen float rock contains fossils of preservation type III as well, but this is the only observed exception; otherwise, only preservation type I was found.

New morphological observations

As illustrated in previous studies (Fig. 5a–c, f, g in Zhang et al. 2006), some fossils in the Jinxian Biota consist of two individuals preserved side-by-side on the same surface and are in contact with each other along a straight margin. One interpretation is that these are individuals that were killed while undergoing asexual reproduction. However, the alternate possibility, that these represent the growth constraint between two adjacent and competing sessile individuals, has not been rejected. Some specimens investigated in this study present a separated inner disc and connected outer apron (Fig. 9a, b, d, e). The annuli in the outer apron are continuous and may have a curvature apparently distinguishable from that of the split inner discs (Fig. 9d). This is different from contacting discoid Ediacaran fossils (e.g., Fig. 15B in Gehling et al. 2000 and Fig. 2C in Grazhdankin and Gerdes 2007) and microbial colonies (e.g., Plate 13, Fig. 8 in Gerdes et al. 1993), in which the contacting bodies are completely separated by the boundary, and the annuli in each disc maintain the same curvature because of the radially expanding nature of growth. For this reason, it is suggested here that these specimens are displaying binary fission.

Based on a series of specimens, a complete process of binary fission can be reconstructed (Fig. 9d–i; details see “Reconstruction”). In light of this concept, those specimens that show two unequally sized bodies contacting along a straight margin may be understood as budding individuals (Fig. 9j–l). Furthermore, those irregularly deformed specimens, which are markedly more abundant in the Yangtun section than in the other sections, may also represent poorly preserved individuals under fission. For instance, the so-called *Quadratimedusa liaoningensis* demonstrated by Wang (1991, Fig. 11 in Plate I; also



◀ **Fig. 4** Different forms and deformations of the discoid fossils in the Jinxian Biota. **a** A specimen showing possible folding on the edge, No. 10231. **b** Nonparallel long axes of the inner and outer annuli, No. 10236. **c** Radial wrinkles, No. 10026. Dome-shaped fossils, **d** No. 10310, **e** No. 10166. **f** A specimen crosscuts the sedimentary bedding at a high angle, No. 10200. **g** No. 10408. The *arrows* indicate a broad and blunt wrinkle, which may be derived from a belt with an abnormal curvature on the fossil umbrella. **h** Severely skewed annuli, No. 10102. **i** A normal shape with a central pimple, No. 10204. The *arrow* indicates a broad annulus whose origin (from a softer or stiffer belt) is difficult to determine with certainty. **j** An *irregular shape*, No. 20330. **k** A *triple-lobed* or *clover-shaped* form, No. 20185. **l** A *heart-shaped* form, No. 20031. **m** A *clover-shaped* form, No. 20317. **n** A *sausage-shaped* specimen, No. 20180. **o**, **p** The same specimen shows an annular or spiral relief in different angles of illumination, No. 10059

shown in Fig. 2-1 in Tang et al. 2009) is clover-shaped with continuous outer annuli, similar to the specimen presented in Fig. 4m, whereas its central part is clearly separated into four quarters.

Another group of Jinxian discoid fossils, which may have been ignored by previous researchers, caught our attention during the field observations. These fossils are generally elliptical (Fig. 10) and show comparable size and preservation to the “normal” discs in the same fossil horizon (e.g., Fig. 10b). However, different from the discrete “normal” discs, these fossils lack any annular or radial relief structures and always occur massively, forming a flat surface. Nevertheless, oriented wrinkles may be present in some specimens of preservation type I (Fig. 10b, d), while in some specimens of preservation type III, there may be a vague color differentiation between the inner and outer parts of the disc (Fig. 10a, c). Until now, these fossils were only known as preservation types I and III. It is hard to determine their identity based on the currently available information, but they are expected to have a certain relation to the discrete, relief-bearing discs. Because we do not have much information regarding this new form of discoid fossils, throughout the rest of this text the term “discoid fossils” will designate the relief-bearing discs only, if the description “relief-lacking” is not emphasized.

Discussion

Taphonomy

Before burial

According to the preservation described above, the discoid fossil organisms probably underwent a suspension stage before being buried and fossilized, although the known information

does not allow a further deduction about whether the suspension is related to a certain lifestyle or just the transport and re-deposition processes. The supporting lines of evidence include:

1. These discoid fossils are only preserved within the mudstone layers, i.e., the late sedimentary phase of a turbidite. This is different from the preservation of many sessile organisms, which are more abundantly preserved on bedding planes or in background beds, e.g., sessile organisms in the Ediacara Biota (Narbonne 2005) and sponges in the Chengjiang Biota (Zhao et al. 2009).
2. Many specimens are preserved oblique to the bedding surface. This may be interpreted as a result of the deformation of non-lithified muddy sediments if several adjacent individuals are affected collectively. However, the individual in Fig. 4f, for instance, cannot be interpreted in this way because it crosscuts the bedding surface at a very high angle and shows strongly skewing annuli, whereas on the other side of the same rock sample (ca. 2-cm thick), another individual is preserved nearly parallel to the bedding surface.
3. The morphology of some specimens is hard to interpret in the model of in-situ preservation. One of our specimens is preserved nearly parallel to the bedding plane with the structure that we interpret as folding of the soft body during deposition (Fig. 4a). Similar examples, in which the elliptical outline and the annular reliefs are terminated by a slightly curved cutting edge, were also illustrated by Zhang et al. (2006, Fig. 5E, I) but alternatively interpreted as “inhibition of growth in one direction” (Zhang et al. 2006, p. 173). However, even following this assumption, the absence of the growth inhibitor, e.g., a contacting individual, would indicate that these fossils were very likely buried after transport.

Burial and early diagenesis

After burial, the fossil organisms experienced first the early diagenetic processes, including decay, compaction, and possibly early diagenetic mineralization. The preservation of the Jinxian Biota is similar to the Burgess-Shale-type preservation in the aspect that non-biomineralized organisms are preserved as compacted bodies in rapidly deposited fine-grained sediments (e.g., Orr et al. 1998; Zhao et al. 2009). However, Burgess-Shale-type preservation *sensu stricto* designates those fossils “whose primary taphonomic mode is one of non-mineralizing organisms preserved as carbonaceous compressions (organic preser-

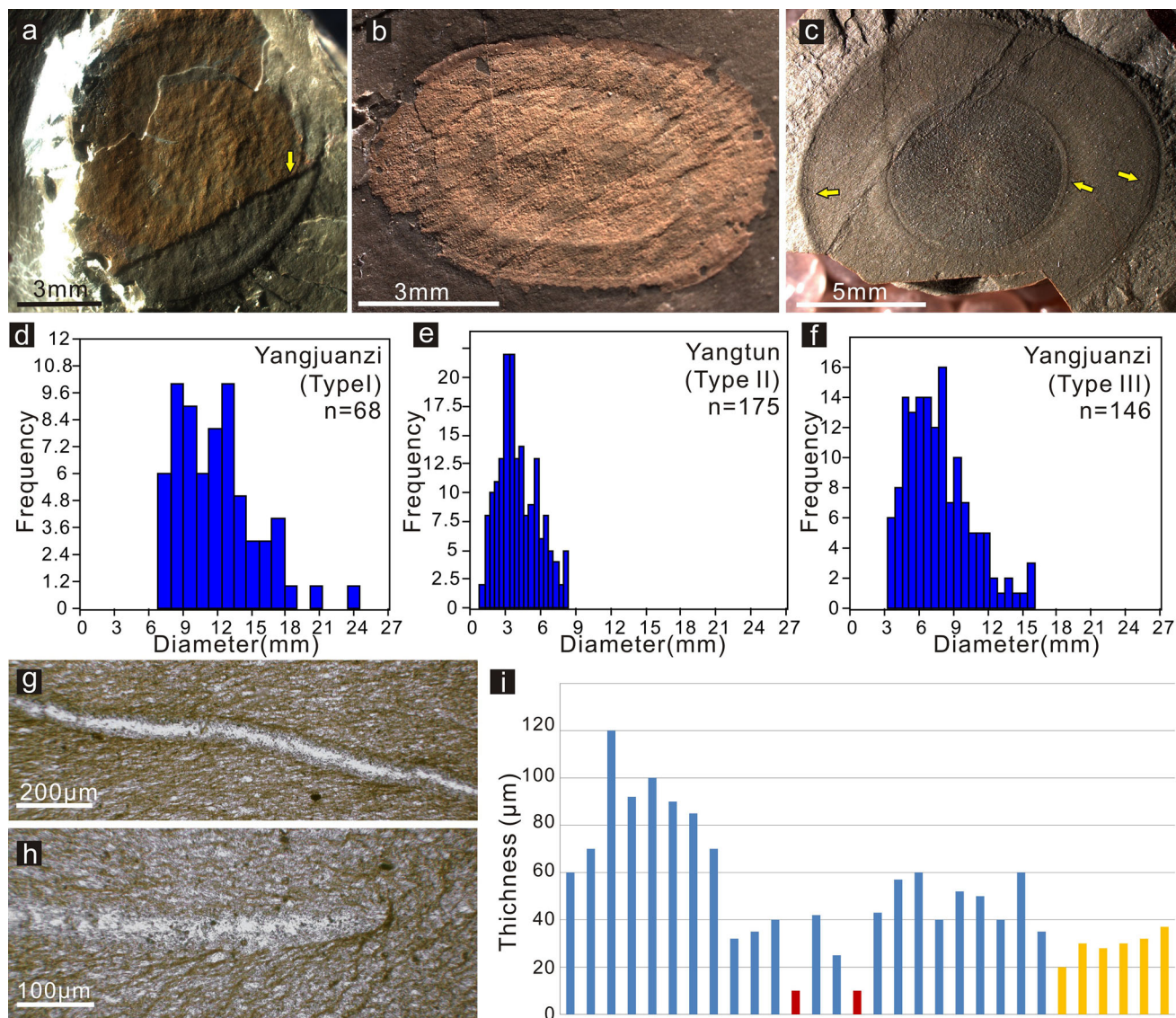


Fig. 5 Three preservation types of the discoid fossils in the Jinxian Biota. **a** Preservation type I; the *arrow* points to where the annular structures vary between the two sides of the mineral sheet, No. 10137. **b** Preservation type II, No. 20139. **c** Preservation type III; the *arrows* point to delicately preserved annular structures, No. 10180. **d–f** Size distribution of the three preservation types. **g–h** Cross sections of the

mineral sheet in preservation type I under an optical microscope. **i** Fossil thickness of different preservation types. The *blue*, *yellow*, and *red bars* represent preservation types I, II, and III, respectively. The two specimens of preservation type III are, in fact, both thinner than 10 μm

vation) in fully marine sediments” (Butterfield 1995, p. 2), whereas the fossils from the Jinxian Biota do not show any direct evidence of primary organic preservation.

Some researchers have detected carbon signals in the fossils of preservation type I (Tang 1997; Zhang et al. 2006). However, our elemental mapping shows that the fossils yield only weak carbon signals equal to those obtained from the host rock, indicating that the previously detected carbon is not necessarily related to the preservation of the discoid fossils. The dark color of the quartz sheets is not associated with any elemental enrichment.

Instead, taking the similarly dark, silty sedimentary layers as a reference (Fig. 3c), this colorization probably originates from the spatial arrangement of clay minerals and quartz grains. Similar to the quartz sheets, the dark color of the silty sedimentary layers cannot be attributed to any elemental abnormality, but in low-magnification SEM images (back-scattered electron mode), the silty parts yield a slightly brighter reflection than the muddy layers (compare Fig. 3i with Fig. 7d–g). This brightness contrast is induced by the accumulation of diagenetic clay minerals in the pore spaces of quartz grains (Fig. 3i).

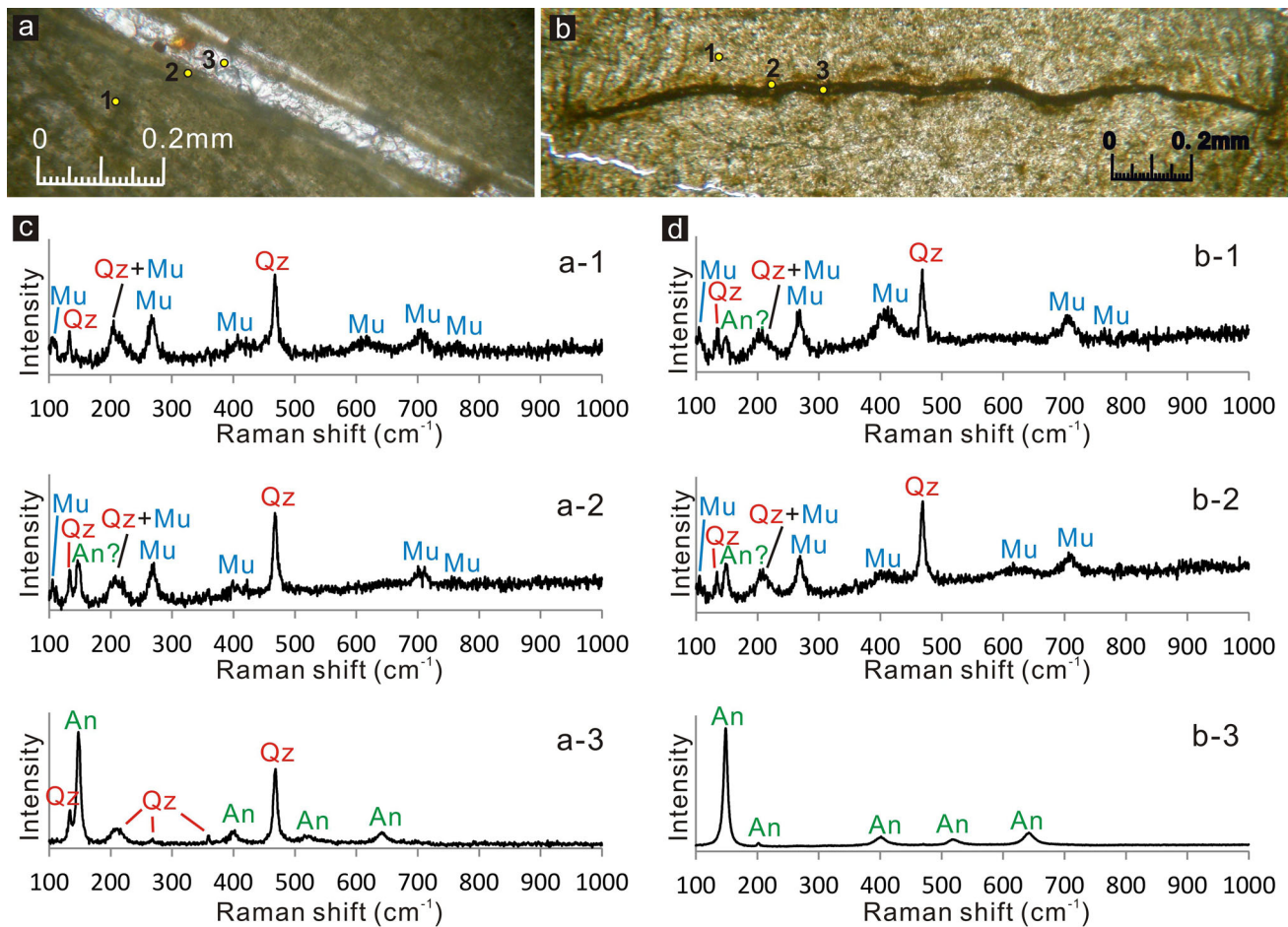


Fig. 6 Raman spectra from fossil cross sections of preservation types I and II. **a, b** Cross section of fossils of preservation type I and II, respectively, under an optical microscope. These two photos are not from the samples that were directly analyzed by Raman spectroscopy; the numbers 1–3 indicate three types of material from which the spectra were taken: the host rock and the edge and center of the fossils, respectively. **c** Raman spectra from qpm-L-1 (transverse

section of a fossil from the Qipanmo section, preservation type I). **d** Raman spectra from yt-L-1 (transverse section of a fossil from the Yangtun section, preservation type II). The spectra denoted a-1, b-1, etc. correspond to the materials marked with the corresponding numbers in **a** and **b**, e.g., a-1 corresponds to the host rock of preservation type I. Abbreviations in spectra interpretation: An anatase, Mu muscovites, Qz quartz

In fact, not only carbonaceous material, but also the early diagenetic minerals with which the organisms first fossilized seem to have disappeared.

The iron enrichment in preservation type III is likely derived from early diagenetic processes instead of being a consequence of later diagenetic precipitation, because preservation type I, which continuously grades into type III within a distance of less than 0.5 m in the same section (Fig. 3a, e–g), was not affected by similar elemental enrichment at all. As a byproduct of the sulfate-reducing anaerobic degradation of organic matter, early diagenetic framboidal pyrite is a common iron mineral involved in exceptional preservation and is commonly associated with the Burgess Shale-type preservational pathway (e.g., Schiffbauer et al. 2014). In the Chengjiang Biota, the decay of some non-mineralized tissues appears to have been

inhibited first by the precipitation of framboidal pyrite, which was then overgrown by Fe-rich clays (Zhu et al. 2005). Pyritization is also presumably involved in the preservation of these Precambrian discoid fossils. However, framboidal pyrite is not directly observed in the specimens of preservation type III.

The fossils of preservation type I are markedly thicker than those of preservation type III (Fig. 5i; Supp. 2). Because fossils of these two preservation types do not show a significant disparity in morphology (Fig. 12), the larger thickness indicates less compaction in early diagenesis, in other words, a faster diagenetic mineralization relative to compaction. However, the quartz sheets now observed in preservation type I are probably not the original product of this rapid mineralization because the discoid fossils do not exhibit the preservation quality of rapidly silicified fossils,

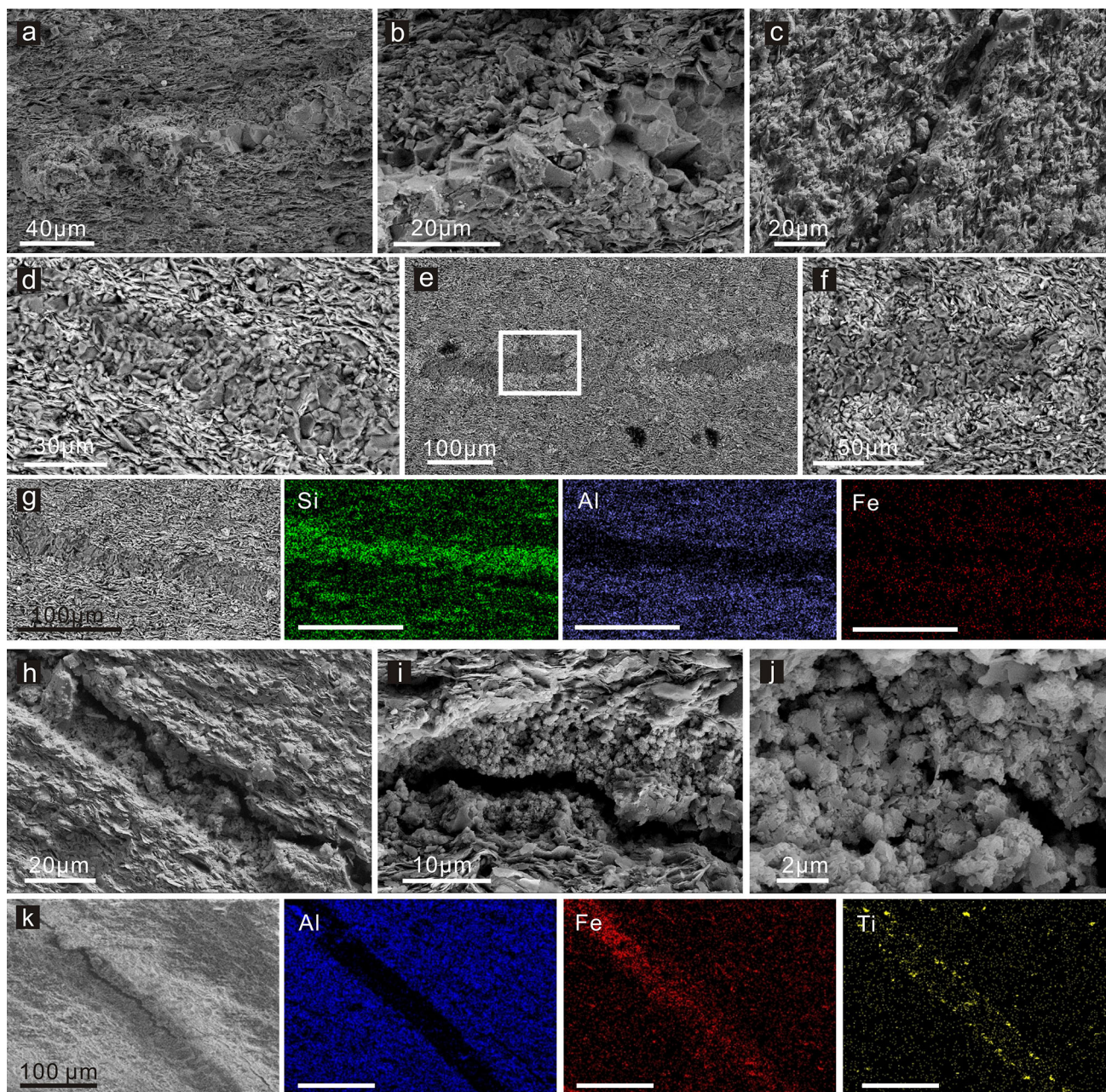


Fig. 7 SEM and X-ray EDS study of the fossil cross sections of the three preservation types. The images in **a–c** and **h–j** were photographed in the secondary electron mode, whereas the images in **d–f** were photographed in the backscattered electron mode. **a, b** Preservation type I, qms-5B. **c** Preservation type III, yjzs-9. **d** Preservation

type I, yjzs-11. **e–f** A fracture in the same rock from which yjzs-11 was obtained. **f** A closer view of the white rectangle in **e**. **g** Elemental mapping of the specimen in **d**. **h–j** Preservation type II, yts-6. **k** Elemental mapping of the transverse section of yt-11 (preservation type II)

and the mineral composition of the quartz sheets was also observed in a fracture filling (Fig. 7e, f).

If these quartz were not the first diagenetic mineral that facilitated the preservation of the discoid fossils, carbonates are here proposed as their precursor. Beside of pyrite and silica, carbonates and phosphates are theoretically the most common minerals allowing the three-dimensional (3-D) replication of the carcass in early diagenesis, whereas

phosphatization is biased to preserve microscopic structures (Allison 1988). Silica replacing a calcite precursor was previously invoked to interpret the formation of the fossiliferous chert nodules in the black shales from the Ediacaran Doushantuo Formation (Xiao et al. 2010). Carbonates were also inferred as the primary diagenetic mineral that enabled the three-dimensional preservation of the gut of *Burgessia* from the Cambrian Burgess Shale

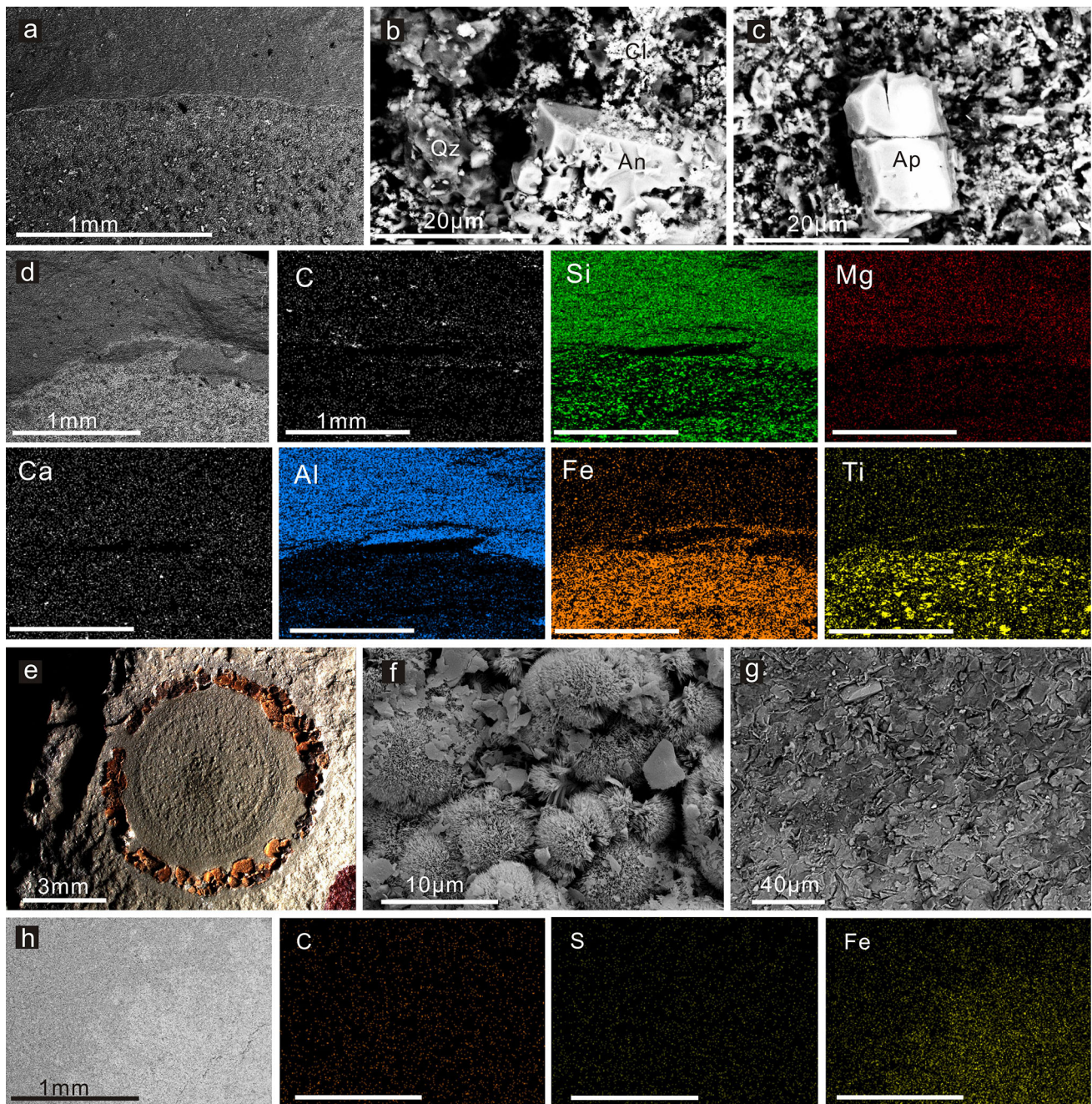


Fig. 8 SEM and EDX study on the fossil surfaces of preservation types II and III. The images in **a–d** were obtained from the specimens of preservation type II. The images in **e–h** were obtained from specimens of preservation type III. **a** The surface of yts-7; the brighter area belongs to the fossil. **b, c** Mineral grains on the fossil surface. **d** Elemental mapping of yts-8; the lower part of each image is the

fossil, ETH = 20.00 kV. **e** A weathered specimen of preservation type III, No. 10226. **f** Weathered part of yjzs-6 under SEM (secondary electron image). **g** A close look at the surface of specimen yjzs-a in the backscattered electron mode. **h** Elemental mapping of the same specimen shown in **g**. The lower-right part is the fossil, EHT = 15 kV. An anatase, Ap apatite, Cl clay minerals, Qz quartz

(Butterfield et al. 2007), whereas these tissues are now preserved with accumulated clay minerals. A low pH will generally promote the dissolution of carbonates and the precipitation of silica. In the Yangjuanzi section, preservation type I is restricted to a 30-cm-thick bed (Fig. 2a), which may reflect a short interval during which the

hydrochemistry was favorable for the precipitation of carbonate in the siliciclastic-dominant environment.

Fossils of preservation type II may have experienced early diagenetic processes similar to those of preservation type I, since they are also preserved with considerable thickness, strong relief, and unstable precursor minerals.

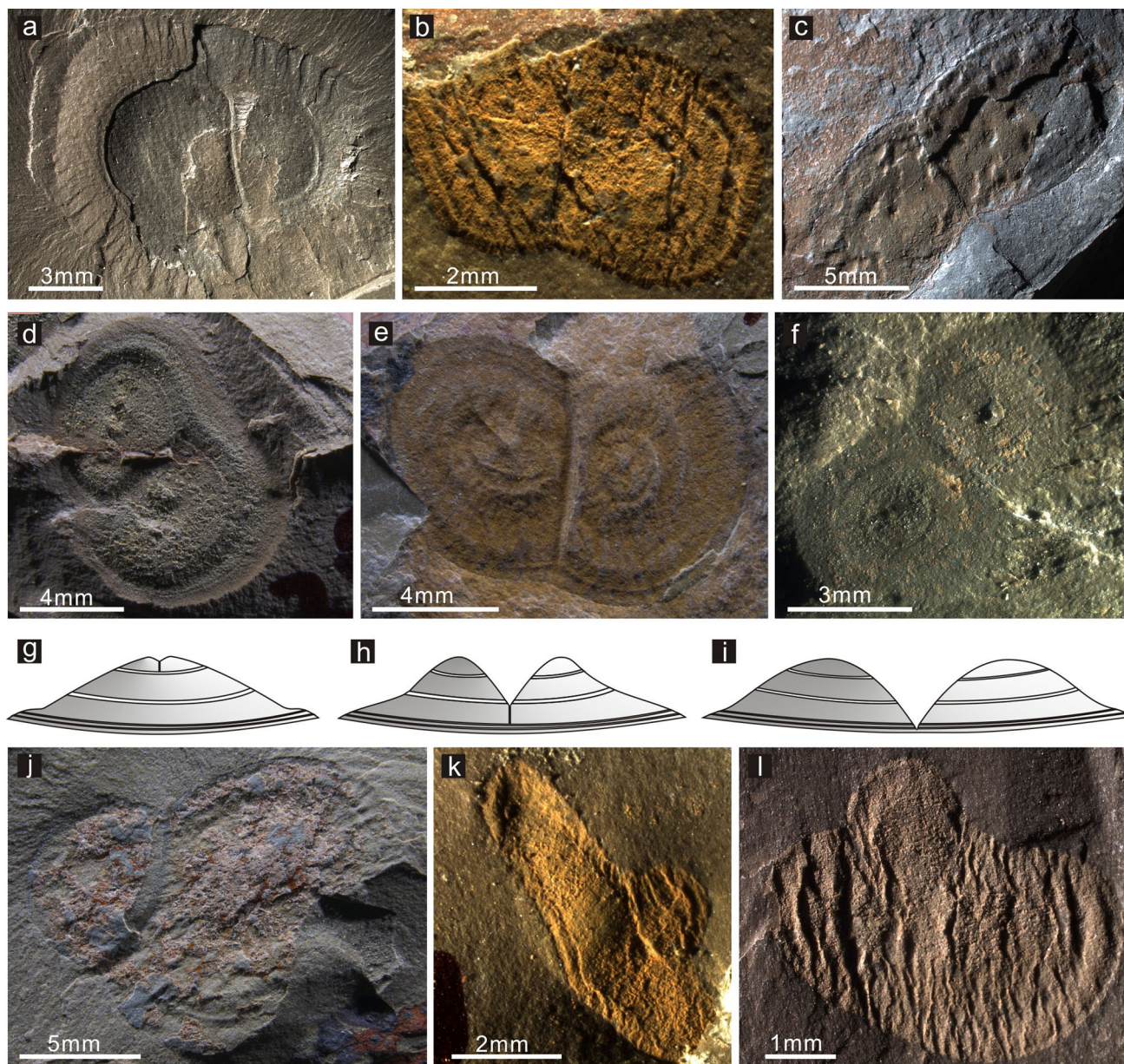


Fig. 9 Binary fission and budding in the discoid fossils of the Jinxian Biota. **a** No. 10033. **b** No. 20298. **c** No. 30003. **d** No. 10230. **e** No. 10327. **f** No. 10160. **g–i** Reconstruction of the fission process based on **d–f**. **j** No. 10311. **k** No. 20313. **l** No. 20157

Late diagenesis and weathering

During these later stages, the early diagenetic minerals underwent alterations to yield the composition observed today. The precursor minerals in preservation type I were replaced by quartz, which may originate from diagenetic fluid or be produced from the diagenetic alteration of clays following the montmorillonite-illite-muscovite/chlorite sequence (Totten and Blatt 1996). Because the surrounding host rock is not apparently silicified, the second source seems to be more probable. In preservation type II, the precursor minerals were dissolved, and the cavities left

behind were filled by minerals precipitated from diagenetic fluids. Morad (1986) has reported that titanium ions can be released from sedimentary detrital Fe–Ti oxides during diagenesis and re-precipitate as anatase to line and fill the pore space of sandstones. This is quite similar to the phenomenon observed in preservation type II. The anatase grains in the silty layers may be a source of titanium ions.

Reconstruction

Except for a few irregular specimens, the discoid fossils are generally circular or elliptical, and many of them do not

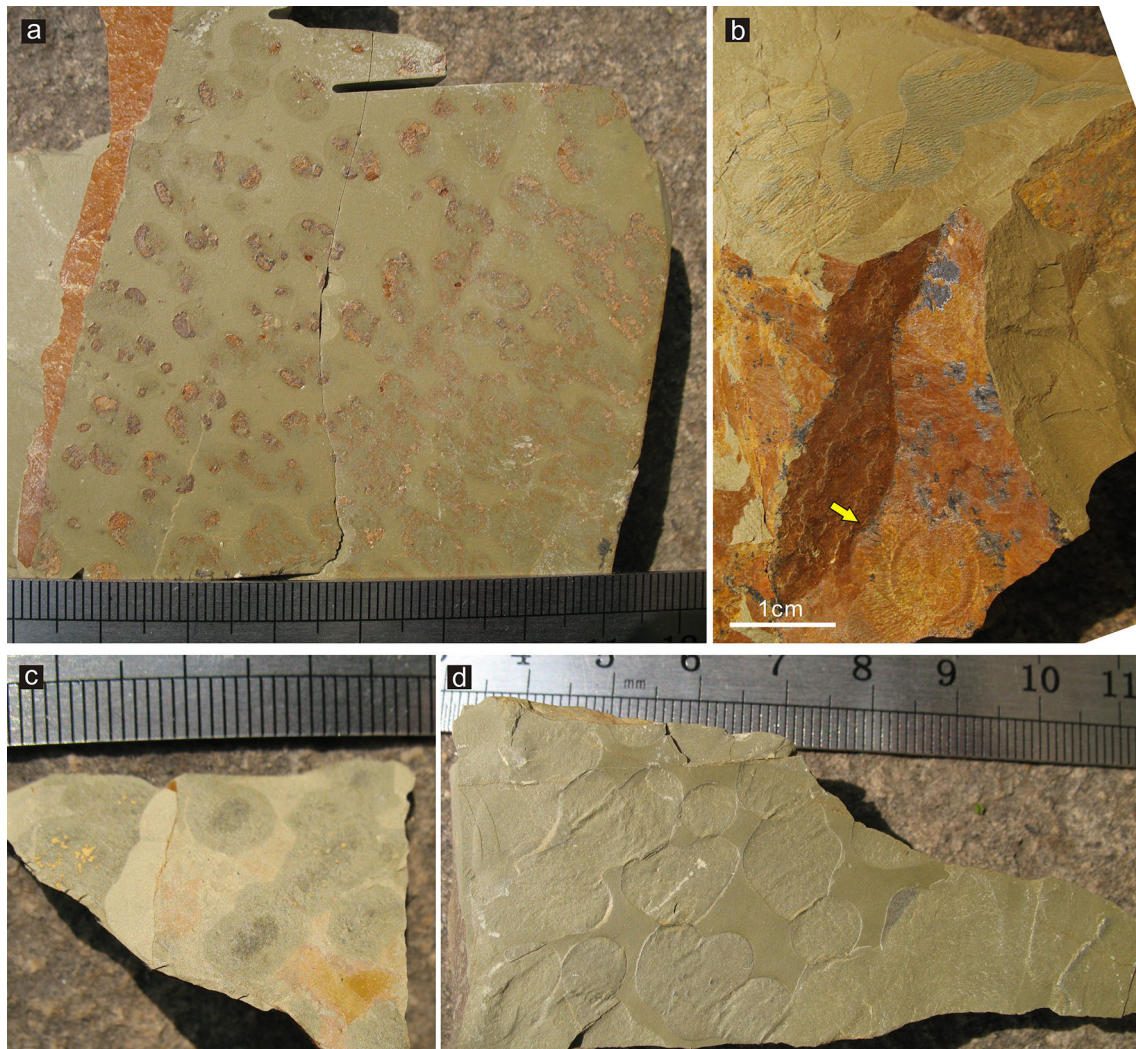


Fig. 10 Relief-lacking discoid fossils in the Jinxian Biota. The specimens in **a–c** were obtained from the Yangjuanzi section. The specimen in **d** was obtained from the Qipanmo section. The specimens in **b** and **d** are of preservation type I, whereas those in

a and **c** are of preservation type III. The *arrow* in **b** points to a relief-bearing discoid fossil, which is preserved together with relief-lacking fossils

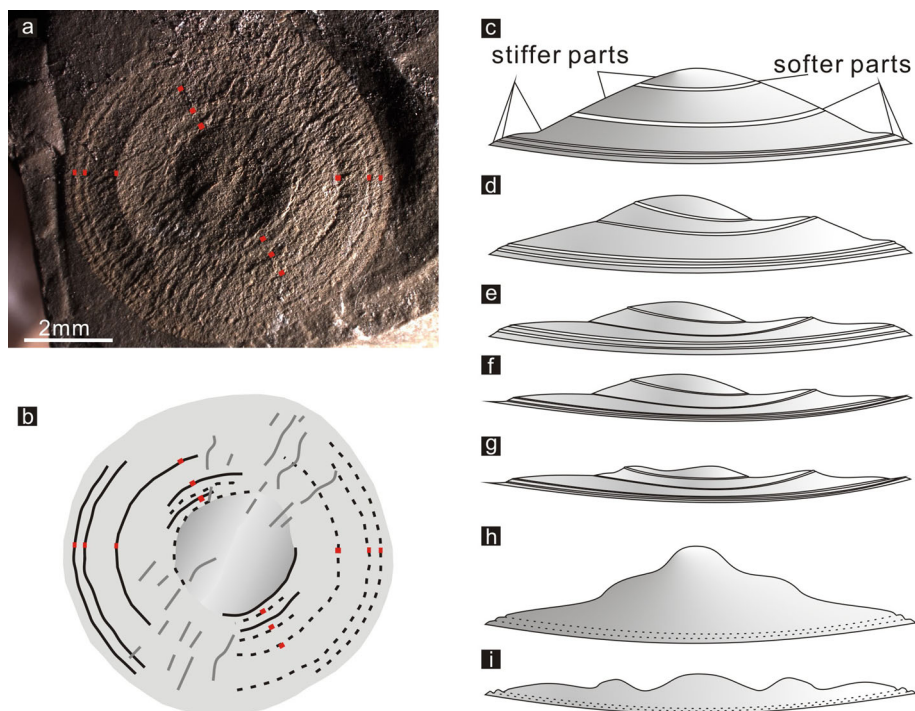
strongly deviate from a circular shape, indicating that the original organisms were probably circular in the two-dimensional (2-D) plane. Although most specimens are compacted, some exceptionally preserved specimens are dome-shaped (Fig. 4d, e). The reliefs and wrinkles in the other compacted fossils indicate a previously existing space below the dome-like body. However, no clues indicate a double-layered structure for the fossil organisms. For these reasons, the fossil organisms are reconstructed in this study as possessing single-layered and umbrella-like bodies.

The concentric annuli in the fossils show a concave relief in one half of the circle and a convex relief in the other half (Fig. 11a, b and other illustrated examples). This type of relief can be correlated to the “concave hemispheric structures” described from decomposing and collapsing medusae on the modern beach (Fig. 2C in

Young and Hagadorn 2010). Thus, when a medusa collapses, one half of the umbrella dents, leaving the other half convex. These structures occur because the area of the umbrella surface is larger than that of the covered bottom. If the material of the umbrella is sufficiently thick or stiff, when part of the umbrella collapses, the remaining part will be squeezed to form a convex relief. This principle is also applicable to the discoid fossils. The relief of the concentric annuli may be regarded as “concave hemispheric structures” that occur repeatedly within one individual.

The concentrically repeated “half convex” deformation can be achieved when assuming that the umbrella is composed of mechanically stiffer rings alternating with softer rings (Fig. 11c–g). Collapse commonly commences first at a certain point in a softer belt. The adjacent stiffer

Fig. 11 Body-plan reconstruction of the discoid fossils. **a** A fossil example, No. 20142. **b** A sketch based on **a**. The *dashed lines* show some fine, concave annuli, whereas the *black solid lines* show some fine, convex annuli. The *grey lines* represent mechanical deformations, and the *red spots* mark corresponding places in **a** and **b**. **c–g** Compaction processes under the assumption that the umbrella is composed of alternating stiffer and softer rings. **h, i** Compaction processes under the assumption that curvature abnormality was the main cause of the concentric reliefs



belt acts like a seesaw, transmitting the deformation immediately to the opposite edge of the belt, where it causes the reverse movement. Fluid movement in the space under the umbrella, if it exists, will promote these processes. In this manner, elegant and sharp annuli with a “half convex” relief can be formed. Then, if the collapse and compaction continue and the softer annuli cannot deform anymore, the stiffer belt will start to wrinkle and generate relatively broader and more irregular relief. Lastly, the relief pattern observed in the discoid fossils will be formed (Fig. 11a).

To interpret the regular annuli in the discoid fossils, an alternative assumption may be that the original umbrella has concentric belts with curvature abnormalities, which could preferentially deform under pressure or gravity force. However, during compaction, it would be difficult for an umbrella with this shape to form elegant and sharp annuli with a “half convex, half concave” relief (Fig. 11h, i). Nevertheless, in part of the fossils, a curvature abnormality may have existed in combination with the alternating stiffer and softer rings. For example, the broad and blunt concentric wrinkles presented in Fig. 4g (arrows) may represent a belt with curvature abnormalities.

In light of this body-plan reconstruction, those specimens featured by binary fission can be arranged (Fig. 9d–f), and the fission process can be interpreted as shown in Fig. 9g–i. The fission appears like a regulated process occurring from top to bottom. The daughter individuals

separate from each other only after each body is fully formed.

As readily detectable morphological structures, the annuli in the discoid fossils have been employed for classification (Hong et al. 1988). However, according to the discussion above, it is necessary to determine first whether an annular relief is derived from an originally soft or stiff belt or from a belt with curvature abnormality. This is sometimes difficult in practice due to information loss during the fossilization process. For example, it may be difficult to tell whether an annulus represents one broad soft belt or a stiff belt between two slender, soft annuli (e.g., arrow in Fig. 4i).

Nevertheless, in this study, we adopted two factors to describe the morphology of the discoid fossils and to explore any possible morphological clustering among them. These are the two ratios: diameter (innermost annulus)/diameter (whole disc) and diameter (outermost annulus)/diameter (whole disc). The preliminary results show an apparent discrepancy between the fossils of preservation type II and those of the other two preservation types (Fig. 12; Supp. 1). The fossil beds in the Yangtun section may represent a different fossil horizon from that in the Qipanmo and Yangjuanzi sections, although the stratigraphic correlation between the two sections is currently not available. The smaller fossil size and higher proportion of irregular individuals in the Yangtun section are more likely an evolutionary or ecological phenomenon rather than a taphonomic bias.

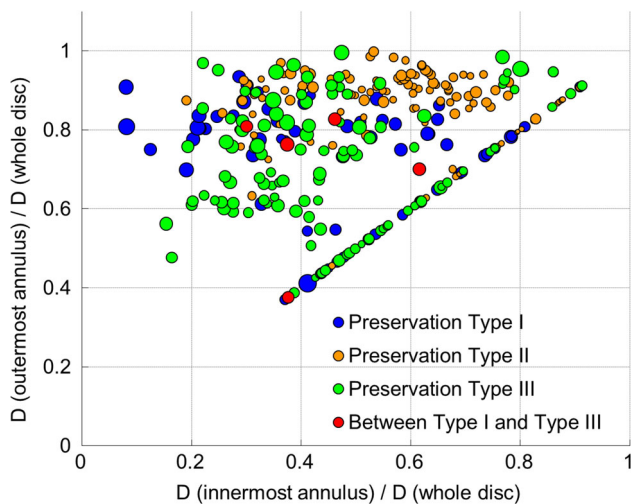


Fig. 12 Bubble diagram showing the clustering of the discoid fossils according to morphological factors. This figure is based on a measurement of 309 specimens, of which 124 were obtained from the Yangtun section (preservation type II) and 185 from the Yangjuanzi Section (67 of preservation type I, 113 of type III, and five of the transitional preservation between type I and III). The coordinate axes represent the ratio of the diameters, whereas the bubble size reflects the size of each specimen [i.e., D (whole disc)]. The diameters were mainly measured along the long axes. In some rare cases in which the long axes were not available, the ratios were calculated based on data of the minor axes. The original data are provided in Supp. 1

Affinity of the medusoid fossils

The studies conducted in the 1980s and 1990s compared the discoid fossils in the Jinxian Biota to cnidarian medusae (Hong et al. 1988; Wang 1991) and Ediacara-type discoid fossils (Niu et al. 1988). However, Zhang et al. (2006, p. 179) concluded that these fossils “do not closely resemble other living or fossil forms” after examining many morphologically similar fossil and living organisms, including Ediacara-type discoid fossils, *Chuaria*-type organic fossils, Precambrian trace fossils, *Horodyskia*, giant bacteria, giant protists, algae, fungi, lichens, and animals.

Based on the updated observations on the taphonomy and body plan of these fossils, this study does not change the conclusion of Zhang et al (2006). If our reconstruction is correct, the fossil organisms were umbrella-like, composed of alternating stiffer and softer concentric belts and capable of programmed, top-to-bottom fission and budding. These features appear to be unique among the known living and fossil organisms.

Among morphologically similar discoid fossils, the Precambrian carbonaceous compressions which show rigid deformation and (in some cases) fracturing on the fossil surface, e.g., *Chuaria*, are generally reconstructed as spherical or oval vesicles (e.g., Hofmann 1985; Dutta et al.

2006; Xiao et al. 2002; Sharma et al. 2009). *Beltanelliformis* from the basal Cambrian Pusa Shale (Fuentes Section) of Spain belongs to this group of organic fossils. According to previous illustrations, these fossils are preserved as organic films with rigid compactional folding, and occurring discretely, massively, or as a chain (e.g., Brasier et al. 1979; Jensen et al. 2007). However, although not delicately preserved, some newly collected discoid fossils from this *Beltanelliformis* horizon resemble part of the Jinxian fossils, particularly those whose annuli are not well developed (Fig. 13). The massive occurrence of the Cambrian fossils is also reminiscent of that of the relief-lacking discoid fossils in the Jinxian Biota, except that the former fossils do not overlap each other and each maintains a complete elliptic shape, whereas the latter fossils often show interconnection and combination (Fig. 10). Further investigation is required to confirm whether the discoid fossils in the Pusa Shale are related to those in the Jinxian Biota.

Discoid impression fossils from the Ediacara Biota were once suggested as an analogue of the discs in the Jinxian Biota. In fact, Ediacara-type discoid impressions have also been found in rocks much older than the Ediacaran age (e.g., Xing and Liu 1979; Hofmann et al. 1990; Cruse and Harris 1994; Bengtson et al. 2007; Meert et al. 2011). Although these discoid fossils of different ages may have various origins, they are exclusively preserved on the bedding surface of sandstone or siltstone and appear as sessile organisms or their attaching organs buried directly at the living position (MacGabhann 2007). Morphologically, these fossils have neither “half convex, half concave” rings nor any convincing features of fission or budding.

It is also difficult to find any modern analogue for the Jinxian discoid fossils. Single prokaryote cells do not reach the size of centimeters (Bailey et al. 2007). Bacterial colonies with specific shapes require a lab environment for culture, and the resulting forms are less regular than the discoid fossil in the Jinxian Biota (e.g., Lei and Zhang 2008). Some microbial mats may form simple concentric surface patterns, such as “fairy rings” (e.g., Gerdes et al. 1993). The discoid fossils in the Jinxian Biota are different from these mat structures because they show distinct and regular boundaries against the host rocks and features of transport. Giant protists, macroalgae, and macroscopic fungi mostly reproduce by generating spores or gametes (e.g., Adl et al. 2005; Goldstein 2002; Lobban and Harrison 1997; Walker and White 2005) instead of by binary fission, which appears to be less effective. Also, we do not know of any examples from these groups that show a similar body plan to the discoid fossils. In the kingdom Animalia, cnidarian medusa were once preferred as an interpretation of these discoid fossils. Previous studies have shown that

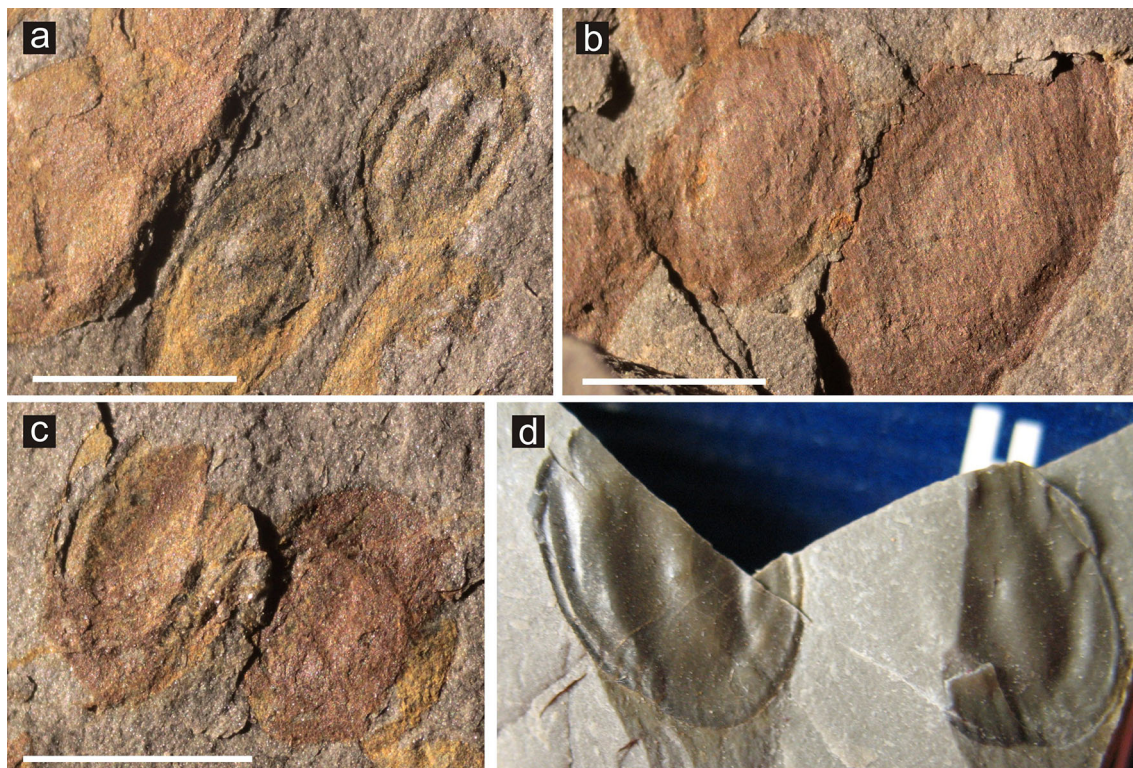


Fig. 13 Similarities between the discoid fossils from the Jinxian Biota and those from the *Beltanelliformis* bed of Lower Cambrian Pusa Shale, Fuentes Section, Spain. The specimens in **a–c** are the Cambrian discoid fossils, *scale bars* represent 5 mm. **d** Two

specimens from the Jinxian Biota with annular structures that are not prominent. Fossils belong to Prof. X. Zhang's collection at Northwest University (China). The lengths of their long axes are between 5 to 10 mm

some hydromedusa can reproduce by longitudinal fission (Russel 1953; Stretch and King 1980), similar to that observed in the discoid fossils. However, the morphological features crucial for determining a medusan affinity, e.g., radial canals, a gastrovascular cavity and tentacles, have not been unequivocally observed in the Jinxian fossils. Additionally, the alternating stiffer and softer concentric annuli of the discoid fossils are not known from modern cnidarian medusa. The primitive animal taxon Placozoa are microbial-mat grazers but can have a free-swimming phase (Thiemann and Ruthmann 1991; Maruyama 2004). Characterized by a simple and flat body plan, placozoans are smaller (1–2 mm in diameter) than the discoid fossils and exhibit a more irregular and asymmetric morphology. In addition, the fission of placozoans appears to be more “unregulated”, merely involving two or three ends of the body moving apart until the connection between them is attenuated and broken (Srivastava et al. 2008).

The available information is still not sufficient to determine the affinity of the discoid fossils in the Jinxian Biota. Even the lifestyle of the fossil organisms is unclear. According to this and previous studies, it is only known that the fossils were transported before burial. Despite of

this, a conclusion of neither a sessile nor a floating lifestyle could be drawn with sufficient support. However, there is a great probability that these fossils represent eukaryotes instead of prokaryotic colonies. Even an animal affinity should not be excluded. This interpretation is at least as likely as other taxonomic possibilities, considering that the fossil organisms show the combination of the following characteristics: megascopic size, soft body, stable morphology, radial symmetry, possible soma differentiation, and programmed fission and budding.

Conclusion

On the basis of previous studies, this investigation refines the understanding of the taphonomy and body plan of the fossils in the Jinxian Biota. The fossil organisms likely possessed umbrella-like bodies composed of alternating softer and stiffer annuli and were capable of binary fission, budding, and possible multiple fission. These organisms were transported by turbidity currents and were then rapidly buried in the muddy sediments. The post-burial history may have involved a pyrite- and carbonate-related early diagenetic mineralization, which allowed a delicate

preservation of the fossils, whereas the differentiated late diagenesis and weathering altered the fossils into the three types of preservation observed today.

However, the questions that remain unresolved outnumber the resolved ones. Some of the questions that still need to be addressed are: (1) What was the lifestyle of these organisms before they were transported? (2) What is the relationship between the relief-bearing and relief-lacking discs? (3) What is the meaning of the finding that the fossils from the Yangtun section are significantly different from those from the Qipanmo and Yangjuanzi sections in both size and morphology? (4) What is the exact age of the fossils? (5) What is the biological affinity of the fossils? Further efforts are required to deciphering these enigmatic fossils and to better understand the Precambrian biosphere.

Acknowledgments We appreciate Prof. X. Zhang (Northwest University, China) for granting us access to his fossil collection; M. Wang, L. Na, and H. He for the assistance provided in the field; and X. Cheng, C. Wang, E. Zhuo, and Dr. N. Schäfer for the help provided with the laboratory work. The discussions with and suggestions from Dr. Z. Yin, Dr. S. Hu, Dr. M. Lü, Prof. D. Jackson, and Dr. B.A. MacGabhann were enlightening and beneficial. We are also grateful to the reviewers Dr. S. Jensen and Dr. J. Schiffbauer for their encouraging and constructive comments on the manuscripts. The project was supported by the Chinese Academy of Science (KZZD-EW-02-2), the Ministry of Science and Technology of China (2013CB835006), and the National Natural Science Foundation of China. The Courant Research Center of Geobiology—Göttingen (German Excellence Initiative, DFG) and the China Scholarship Council (CSC) are also acknowledged for the financial support provided.

References

- Adl, S.M., A.G.B. Simpson, M.A. Farmer, R.A. Andersen, O.R. Anderson, J.R. Barta, S.S. Bowser, et al. 2005. The new higher level classification of eukaryotes with emphasis on the taxonomy of protists. *Journal of Eukaryotic Microbiology* 52(5): 399–451.
- Allison, P.A. 1988. Konservat-Lagerstätten: Cause and classification. *Paleobiology* 14(4): 331–344.
- Bailey, J.V., S.B. Joye, K.M. Kalanetra, B.E. Flood, and F.A. Corsetti. 2007. Evidence of giant sulphur bacteria in Neoproterozoic phosphorites. *Nature* 445: 198–201.
- Bengtson, S., B. Rasmussen, and B. Krapež. 2007. The Neoproterozoic megascopic Stirling biota. *Paleobiology* 33(3): 351–381.
- Brasier, M.D., A. Perejón, and D.S. José. 1979. Discovery of an important fossiliferous Precambrian-Cambrian sequence in Spain. *Estudios Geológicos* 35: 379–383.
- Butterfield, N.J. 2009. Modes of pre-Ediacaran multicellularity. *Precambrian Research* 173: 201–211.
- Butterfield, N.J. 1995. Secular distribution of Burgess-Shale-type preservation. *Lethaia* 28(1): 1–13.
- Butterfield, N.J., U. Balthasar, and L.A. Wilson. 2007. Fossil diagenesis in the Burgess Shale. *Palaentology* 50(3): 537–543.
- Cao, R., T. Tang, and Y. Xue. 1988. The connection of the Upper Precambrian in N. China with the Sinian system in S. China. *Geological Review* 34(2): 173–178.
- Cruse, T., and L.B. Harris. 1994. Ediacaran fossils from the Stirling Range Formation, Western Australia. *Precambrian Research* 67: 1–10.
- Duan, J., and S. An. 1994. On the subdivision and correlation of Upper Precambrian System in South Liaoning Province, China. *Liaoning Geology* 1–2: 30–43.
- Dutta, S., M. Steiner, S. Banerjee, B.-D. Erdtmann, S. Jeevankumar, and U. Mann. 2006. *Chuarina circularis* from the early Mesoproterozoic Suket Shale, Vindhyan Supergroup, India: Insights from light and electron microscopy and pyrolysis-gas chromatography. *Journal of Earth System Science* 115(1): 99–112.
- Fairchild, I.J., B. Spiro, P.M. Herrington, and T. Song. 2000. Controls on Sr and C isotope compositions of Neoproterozoic Sr rich limestones of East Greenland and North China. *SEPM (Society for Sedimentary Geology)* 67: 297–313. (**Special Publication**).
- Gehling, J.G., G.M. Narbonne, and M.M. Anderson. 2000. The first named Ediacaran body fossils, *Aspidella terranovica*. *Palaentology* 43(3): 427–456.
- Gerdes, G., M. Claes, K. Dunajtschik-Piewak, H. Riege, W. Krumbein, and H.-E. Reineck. 1993. Contribution of microbial mats to sedimentary surface structures. *Facies* 29(1): 61–74.
- Geological Survey Group of Liaoning Province Team 1. 1972. Instruction Book for the 1:200000 Geological map of Fuzhou, Lvshun, Dalian and Dengshahe Region. In Geological Map of Liaoning Province.
- Goldstein, S.T. 2002. Foraminifera: A biological overview. In *Modern Foraminifera*, ed. B.K.S. Gupta, 37–55. New York, Boston, Dordrecht, London, Moscow: Kluwer Academic Publishers.
- Grazhdankin, D., and G. Gerdes. 2007. Ediacaran microbial colonies. *Lethaia* 40(3): 201–210.
- Hofmann, H.J. 1985. The Mid-Proterozoic Little Dal Macrobiota, Mackenzie Mountains, North-West Canada. *Palaentology* 28(2): 331–354.
- Hofmann, H.J., G.M. Narbonne, and J.D. Aitken. 1990. Ediacaran remains from intertillite beds in northwestern Canada. *Geology* 18(12): 1199–1202.
- Hong, Z., Z. Huang, and X. Liu. 1991. *Geology of Upper Precambrian in southern Liaodong Peninsula*. Special Reports on Geology from the Ministry of Geology and Mineral Resources, People's Republic of China. Beijing: Geological Publishing House.
- Hong, Z., Z. Huang, X. Yang, J. Lan, B. Xian, and Y. Yang. 1988. Medusoid fossils from the Sinian Xingmencun Formation of southern Liaoning. *Acta Geologica Sinica* 62(3): 200–209.
- Hong, Z., Y. Yang, and X. Liu. 1990. Archaeocyathid fossils from the Lower Cambrian Jianchang Formation of the southern Liaodong Peninsula. *Geological Review* 36(6): 558–563.
- Jensen, S., T. Palacios, and M.M. Mus. 2007. A brief review of the fossil record of the Ediacaran-Cambrian transition in the area of Montes de Toledo-Guadalupe, Spain. *Geological Society, London, Special Publications* 286(1): 223–235.
- Lei, M., and X. Zhang. 2008. Research on morphology of modern microbial colonies and the implication for interpreting the affinities of the Ediacara Biota. *Acta Palaentologica Sinica* 47(4): 468–476.
- Lobban, C.S., and P.J. Harrison. 1997. *Seaweed life histories*. In *Seaweed Ecology and Physiology*, 32–47. Cambridge: Cambridge University Press.
- MacGabhann, B.A. 2007. Discoidal fossils of the Ediacaran biota: A review of current understanding. In *The Rise and Fall of the Ediacaran Biota*, eds. P. Vickers-Rich, and P. Komarower,

- 297–313. London: Geological Society (London, Special Publications).
- Maruyama, Y.K. 2004. Occurrence in the field of a long-term, year-round, stable population of placozoans. *The Biological Bulletin* 206(1): 55–60.
- Meert, J.G., A.S. Gibsher, N.M. Levashova, W.C. Grice, G.D. Kamenov, and A.B. Ryabinin. 2011. Glaciation and ~770 Ma Ediacara (?) fossils from the Lesser Karatau microcontinent, Kazakhstan. *Gondwana Research* 19(4): 867–880.
- Morad, S. 1986. SEM study of authigenic rutile, anatase and brookite in Proterozoic sandstones from Sweden. *Sedimentary Geology* 46(1–2): 77–89.
- Narbonne, G.M. 2005. The Ediacara Biota: Neoproterozoic origin of animals and their ecosystems. *Annual Reviews of Earth and Planetary Sciences* 33: 421–442.
- Narbonne, G.M., S. Xiao, and G.A. Shields. 2012. The Ediacaran Period. In *The Geological Time Scale 2012*, eds. F.M. Gradstein, J.G. Ogg, M. Schmitz, and G. Ogg, 413–435. Elsevier.
- Niu, S., M. Wang, and H. Dong. 1988. The discovery of the fossil medusoids (genera *Cyclomedusa* etc., Cnidaria) from Xingmincun formation, Sinian system in Jinxian County, Liaoning Province, China and its significance. *Bulletin of the Tianjin Institute of Geology and Mineral Resources, Chinese Academy of Geological Sciences* 19: 75–86.
- Orr, P.J., D.E.G. Briggs, and S.L. Kearns. 1998. Cambrian Burgess Shale animals replicated in clay minerals. *Science* 281: 1173–1175.
- Ou, Z., and F. Meng. 2013. Precambrian “medusoid” fossils from the Xingmincun Formation of southern Liaoning Province: A new insight. *Acta Micropalaeontologica Sinica* 30(1): 99–106.
- Peterson, K.J., B. Waggoner, and J.W. Hagadorn. 2003. A fungal analog for Newfoundland Ediacaran fossils? *Integrative and Comparative Biology* 43(1): 127–136.
- Qiao, X., L. Gao, and Y. Peng. 2001. *Neoproterozoic in Paleo-Tanlu Fault Zone: Catastrophe, Sequences and Biostratigraphy*, 128. Beijing: Geological Publishing House.
- Russell, F.S. 1953. Introduction: The structural characters of Medusae. In *The medusae of the British Isles*, 1–21. Cambridge: Cambridge University Press.
- Schiffbauer, J.D., S. Xiao, Y. Cai, A.F. Wallace, H. Hua, J. Hunter, H. Xu, Y. Peng, and A.J. Kaufman. 2014. A unifying model for Neoproterozoic–Palaeozoic exceptional fossil preservation through pyritization and carbonaceous compression. *Nature Communications* 5: 5754.
- Sharma, M., S. Mishra, S. Dutta, S. Banerjee, and Y. Shukla. 2009. On the affinity of *Chuaria-Tawuia* complex: A multidisciplinary study. *Precambrian Research* 173(1–4): 123–136.
- Shields, G.A. 2002. ‘Molar-tooth microspar’: A chemical explanation for its disappearance ~750 Ma. *Terra Nova* 14: 108–113.
- Shields-Zhou, G.A., A.C. Hill, and B.A. MacGabhann. 2012. The Cryogenian Period. In *The Geological Time Scale 2012*, eds. F.M. Gradstein, J.G. Ogg, M. Schmitz, and G. Ogg, 393–411. Elsevier.
- Srivastava, M., E. Begovic, J. Chapman, N.H. Putnam, U. Hellsten, T. Kawashima, A. Kuo, et al. 2008. The *Trichoplax* genome and the nature of placozoans. *Nature* 454(7207): 955–960.
- Stretch, J.J., and J.M. King. 1980. Direct fission: An undescribed reproductive method in hydromedusae. *Bulletin of Marine Science* 30(2): 522–525.
- Tang, F. 1997. Megafossils and stratigraphy of the Late Precambrian strata in eastern margin of the North China Platform. Unpublished PhD thesis, 56. Beijing: Chinese Academy of Geological Sciences.
- Tang, F., C. Yin, L. Gao, P. Liu, Z. Wang, and S. Chen. 2009. Macrofossil records of the Neoproterozoic in the eastern of North China Craton: An implement of Neoproterozoic biostratigraphy. *Geological Review* 55(3): 305–317.
- Thiemann, M., and A. Ruthmann. 1991. Alternative modes of asexual reproduction in *Trichoplax adhaerens* (Placozoa). *Zoomorphology* 110(3): 165–174.
- Totten, M.W., and H. Blatt. 1996. Sources of silica from the illite to muscovite transformation during late-stage diagenesis of shales. *SEMP* 55: 85–92 (Special Publication).
- Walker, G.M., and N.A. White. 2005. Introduction to fungal physiology. In *Fungi: Biology and Applications*, ed. K. Kavanagh, 1–35. Chichester: Wiley.
- Wang, M. 1991. Sinian medusas from Dalian, Liaoning Province, China. *Journal of Changchun University of Earth Science* 21(3): 259–312.
- Xiao, S., J.D. Schiffbauer, K.A. McFadden, and J. Hunter. 2010. Petrographic and SIMS pyrite sulfur isotope analyses of Ediacaran chert nodules: Implications for microbial processes in pyrite rim formation, silicification, and exceptional fossil preservation. *Earth and Planetary Science Letters* 297(3–4): 481–495.
- Xiao, S., B. Shen, Q. Tang, A.J. Kaufman, X. Yuan, J. Li, and M. Qian. 2014. Biostratigraphic and chemostratigraphic constraints on the age of Early Neoproterozoic carbonate successions in North China. *Precambrian Research* 246: 208–225.
- Xiao, S., X. Yuan, M. Steiner, and A.H. Knoll. 2002. Macroscopic carbonaceous compressions in a terminal Proterozoic shale: A systematic reassessment of the Miaohé Biota, South China. *Journal of Paleontology* 76(2): 347–376.
- Xing, Y., and G. Liu. 1979. Coelenterate fossils from the Sinian System of southern Liaoning and its stratigraphical significance. *Acta Geologica Sinica* 3: 168–172.
- Xing, Y. et al. 1989. *Upper Precambrian in China*. Stratigraphy of China, vol. 3, 314. Beijing: Geological Publishing House.
- Xue, Y., R. Cao, T. Tang, L. Yin, C. Yu, and J. Yang. 2001. The Sinian stratigraphic sequence of the Yangtze region and correlation to the Late Precambrian strata of North China. *Journal of Stratigraphy* 25(3): 207–234.
- Yang, S. 1984. Late Precambrian microplant fossils from southern Liaodong Peninsula and their stratigraphic significance. *Bulletin of the Shenyang Institute of Geology and Mineral Resources, Chinese Academy of Geological Sciences* 10: 107–130.
- Yang, D., W. Xu, Y. Xu, Q. Wang, F. Pei, and F. Wang. 2012. U-Pb ages and Hf isotope data from detrital zircons in the Neoproterozoic sandstones of northern Jiangsu and southern Liaoning Provinces, China: Implications for the Late Precambrian evolution of the southeastern North China Craton. *Precambrian Research* 216–219: 162–176.
- Young, G.A., and J.W. Hagadorn. 2010. The fossil record of cnidarian medusae. *Palaeoworld* 19(3–4): 212–221.
- Zhang, X., H. Hua, and J. Reitner. 2006. A new type of Precambrian megascopic fossils: The Jinxian biota from northeastern China. *Facies* 52: 169–181.
- Zhao, F., J.-B. Caron, S. Hu, and M. Zhu. 2009. Quantitative analysis of taphofacies and paleocommunities in the Early Cambrian Chengjiang Lagerstätte. *Palaios* 24(12): 826–839.
- Zheng, W., J. Yang, T. Hong, X. Tao, and Z. Wang. 2004. Sr and C isotopic correlation and the age boundary determination for the Neoproterozoic in the southern Liaoning and northern Jiangsu—northern Anhui Provinces. *Geological Journal of China Universities* 10(2): 165–178.
- Zhu, M., L.E. Babcock, and M. Steiner. 2005. Fossilization modes in the Chengjiang Lagerstätte (Cambrian of China): Testing the roles of organic preservation and diagenetic alteration in exceptional preservation. *Palaeogeography, Palaeoclimatology, Palaeoecology* 220: 31–46.